Jurnal Teknologi Reaktor Nuklir

Tri Dasa Mega

Journal homepage: jurnal.batan.go.id/index.php/tridam/index

# Investigation of Natural Circulation Flow Under Steady-State Conditions Using a Rectangular Loop

**Iwan Roswandi[1], Dimas[2], Hyundianto Arif Gunawan[1], Arif Adtyas Budiman[1], Almira Citra Amelia[1], Sanda[1], Hendro Tjahjono[1], Mulya Juarsa[1,*].**

*[1]Nuclear Reactor Thermal-Fluids System Development (NRTFSyDev.) Research Group, Research Center for Nuclear Reactor Technology, Research Organization for Nuclear Energy, National Research and Innovation Agency (BRIN), KST. B.J. Habibie, Setu, Tangerang Selatan 14314, Banten, Indonesia*

*[2]Bachelor Student on Department of Mechanical Engineering, Faculty of Engineering, Universitas Negeri Jakarta, Kampus A UNJ Gedung L, Jl. Rawamangun Muka Raya, Kec. Pulo Gadung, Kota Jakarta Timur, DKI Jakarta 13220, Indonesia*

**ARTICLE INFO**

*Article history*:

Received: May 2nd, 2024
Received in revised form: June 9th, 2024
Accepted: June 10th, 2024

*Keywords:*

NPP
Grashof Number
FASSIP-05
NCL
Pasive Cooling

**A B S T R A C T**

Passive safety systems, particularly during active system failures, have become a significant concern. Understanding natural circulation phenomena is crucial for developing passive cooling systems in nuclear power plants. With its significant findings, this study examines the flow patterns under steady-state conditions and assesses the Grashof number. The experimental approach involved maintaining temperature differences of 60 °C, 70 °C, 80 °C, and 90 °C for 3 hours, with three replications. The temperature alterations impact water's physical properties, such as density, viscosity, and specific heat. The calculations reveal that the minimum Grashof number occurs at 60 °C is $2.49\times10^{12}$, while the maximum is observed at 90 °C is $9.42\times10^{12}$, with an $R^2$ value of 0.96533. The observation of turbulent flow patterns during each temperature fluctuation, which aligns with previous research on the $Re_{ss}$ value of $Gr_m/N_G$, has significant implications for the design and operation of passive safety systems in nuclear power plants.



## 1. INTRODUCTION

The Fukushima Daiichi nuclear power plant accident has provided crucial lessons for researchers and nuclear reactor designers worldwide. Japan experienced a 9.0 magnitude earthquake, one of the most powerful in recorded history, followed by a devastating tsunami, resulting in significant damage at the Fukushima Daiichi plant. The earthquake caused severe structural damage and a complete power outage in all reactor units, resulting in a Station Blackout (SBO) and the failure of active cooling functions [1–3].

In light of such events, implementing passive cooling systems in all types of nuclear power plants (NPPs) becomes essential as a preventive measure to maintain reactor safety during emergencies when active cooling systems fail. Passive cooling systems rely on natural processes without requiring external power, utilizing the natural circulation of fluid driven by density differences. In these systems, fluid in the hot region becomes less dense and rises due to buoyancy forces, while fluid in the cold region becomes denser and sinks, creating a natural convection loop. This passive mechanism ensures safer and more reliable thermal management in power plants [4, 5].

The Research Organization for Nuclear Energy (ORTN), part of the National Research and Innovation Agency (BRIN), has developed various experimental facilities to study natural circulation. One of them is the Passive Simulation System

* Corresponding author. Tel./Fax.: 081384486838
E-mail: iwan032@brin.go.id and mulya.juarsa@brin.go.id

Facility (FASSIP), located within the Thermal-Hydraulic Experiment Laboratory of the Nuclear Thermal-Fluid Reactor System (NRTFSys.) research group. This laboratory operates under the Research Center for Nuclear Reactor Technology (PRTRN), supervised by ORTN BRIN.

In 2014, the construction of the NC-Queen experimental facility marked a significant milestone in our understanding of heat transfer in the natural circulation phenomena. The facility comprises ¾-inch pipes measuring 2.7 meters in length and 0.5 meters in width, with a 1.4-meter distance between the cooler and heater. Initial calculations revealed an astounding 81% increase in the average mass flow rate as the temperature rose from 70 °C to 90 °C [6]. Additionally, FASSIP-01 mod 1, established in 2016, continued to provide valuable insights, featuring a medium-sized vertical rectangular loop made of SS 304 material with a 1-inch diameter, 3.5-meter width, and 6-meter height, divided into 32 sections. Observations indicated that the circulation flow rate increased from 0.04 to 0.06 kg/s with a rise in heater power from 1000 W to 2000 W [7]. These findings underscore the potential for significant advancements in passive cooling systems, it inspiring to continue the research and push the boundaries of our understanding.

FASSIP-02 was constructed in 2018 and consists of a 43.7-meter long, 1-inch diameter piping system made of SS 304. The temperature difference (ΔT) between the inlet and outlet pipes increased as the heater tank temperatures rose. The facility was supported by U-shaped heat exchangers and designed to study single-phase and two-phase flows during natural circulation in large-scale facilities [8]. In 2021, the NRTFSys research group developed FASSIP-03 NT, featuring ultrafine bubble fluid. This fluid is used to investigate the performance of heat removal from hot areas to cold areas and to study helical heat exchangers on both the Heating Tank System (HTS) and Cooling Tank System (CTS) to enhance heat transfer efficiency [9]. In 2022, FASSIP-04 was constructed, which revealed bubble formation from a 5.6 kW heater operating at 105 °C during the commissioning process [10].

PRTRN has also established an advanced rectangular loop for natural circulation testing, named FASSIP-05, with innovations such as pressurized working fluids and adjustable loop inclination angles [11]. A reliability investigation conducted in 2023 assessed the performance of the FASSIP-05 heater and cooler, finding that the heater performed reliably, while the cooler's performance was suboptimal [12]. This study aims to determine the flow regime type during steady-state conditions through a literature review and temperature distribution calculations in a unique experimental setup. The working pressure was kept at 1 bar and operated without a flow meter, a departure from previous research. These conditions distinguish this study and enhance the understanding of data processing to determine natural circulation flow regimes in passive cooling loops for nuclear reactors without relying on a flow meter.

## 2. THEORY

### 2.1 Grashof Number in Natural Circulation Loop

The Grashof number (Gr) is a dimensionless parameter crucial in fluid dynamics, particularly in the analysis of natural circulation systems. It represents the buoyancy ratio to viscous forces within a fluid flow, providing profound insight into the flow regime. In the context of the FASSIP-05 system, the Grashof number is used to assess the flow regime under varying temperature conditions. Higher Grashof numbers indicate stronger buoyancy than viscous forces, suggesting a turbulent flow regime. In this study, the Grashof number varied with temperature changes, offering a detailed view of the natural circulation phenomenon within the system. It's important to note that a Grashof number less than $10^3$ indicates laminar flow, while a value greater than $10^9$ suggests turbulent flow. This relationship between the Grashof number and flow regime allows a precise understanding of the system's behavior. Transitional flow regimes occur between these two extremes [13].

### 2.2 Thermal Expansion

Thermal expansion, a fundamental physical property, is crucial in the FASSIP-05 system. Its understanding is vital, to predicting water behavior within the natural circulation loop. As water temperature varies, its density and buoyancy forces change, directly impacting natural circulation in significant way. The thermal expansion coefficient, is integrated into Grashof number calculations. This coefficient quantifies the extent of density changes due to temperature, facilitating the determination of flow regimes based on the balance between buoyancy and viscous forces [14].

### 2.3 The Physical Properties of Water

The physical properties of water, especially under varying thermal and pressure conditions, are critical in analyzing natural circulation systems. In 1993, Crabtree & Siman-Tov compiled correlations

for the physical properties of water within the 20 °C – 300 °C temperature range and saturated pressure range of 0.0025 - 8.5 MPa, partly based on ASME steam tables. These correlations ensure accurate predictions of water behavior, with discrepancies in the correlation of physical properties generally below 0.7%, except for saturated vapor density, which shows a deviation of 1.76% [15].

### 2.4 The Reynolds Number

The Reynolds number (Re) plays a crucial role in characterizing fluid flow, particularly in determining whether the flow is laminar, transitional, or turbulent. In the context of natural circulation, where flow is driven by temperature-induced density variations, the Reynolds number is instrumental in confirming the flow regime predicted by the Grashof number. In this research, the flow regimes were initially assessed using the Grashof number. These findings were then further validated using the correlation proposed by P.K. Vijayan in 2002. It is worth noting that this correlation is widely recognized among researchers for its role in establishing flow patterns in natural circulation loops [16].

### 2.5 The Surface Roughness and Friction Factor in Stainless Steel Pipes

The FASSIP-05 system, a crucial component of our study, utilizes stainless steel pipes. This choice significantly impacts the system's performance, with surface roughness playing a pivotal role. Higher surface roughness, for instance, can lead to increased frictional forces, resulting in more significant energy losses and potentially reduced fluid flow efficiency. Churchill's equation calculates the friction factor (f) in turbulent pipe flow, considering the surface roughness of the pipe material. The relative roughness factor (ε/D) is a key variable in this equation, where a smaller value indicates a smoother pipe surface and, consequently, lower friction levels [17]. With these detailed analyses, this study is not just about understanding natural circulation flow regimes in passive cooling systems. The research study aims to significantly advance nuclear reactor safety and thermal management strategies, highlighting their importance and impact.

## 3. METHODOLOGY

### 3.1 Experiment Setup

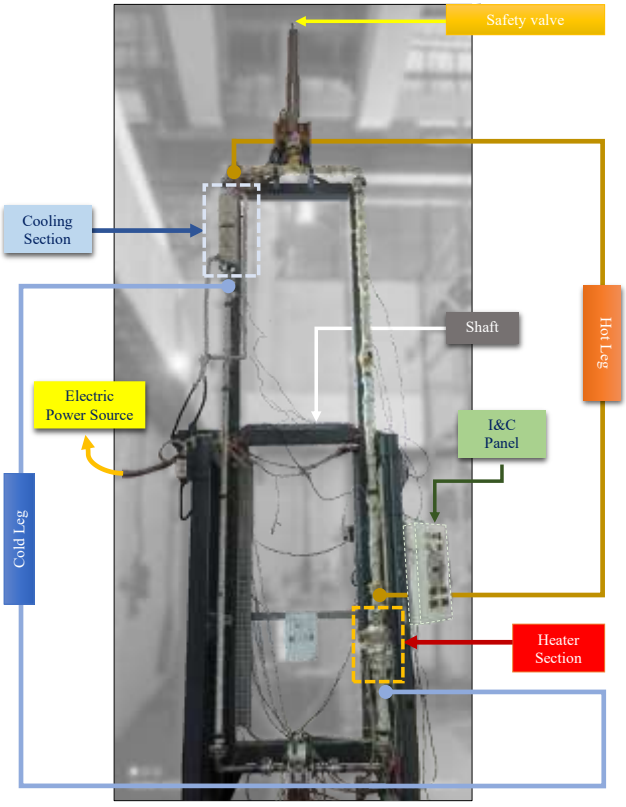


**Fig. 1.** Loop of the FASSIP-05.

The FASSIP-05 is a medium-scale passive cooling facility featuring a rectangular closed-loop geometry constructed from stainless steel 304 sch 160 type pipes with a diameter of 1 inch, a width of 1 meter, and a height of 4 meters. The height difference between the heater and the cooler is 2.67 meters, creating an effective NCL. The heating system comprises four Elstein Infrared Panel Heaters (1000W FSR) positioned at the bottom of the vertical loop (hot leg), forming a bend heater to heat the water inside the pipes, simulating a power reactor's heat generation. The heat from the heaters increases the water temperature, reducing its density and causing it to rise due to buoyancy forces. At the top of the vertical loop (cold leg), a cooler functions as a heat exchanger, utilizing a water tank wound with helical copper pipes through which refrigerant 134a flows, driven by a 2 HP condenser. This setup cools the water in the pipes, increasing its density and causing it to descend through the cold leg, establishing a continuous natural circulation loop essential for passive cooling in reactor systems. Figure 2 illustrates the instrumentation and control diagram of FASSIP-05, detailing the setup and monitoring systems used during the experiments.

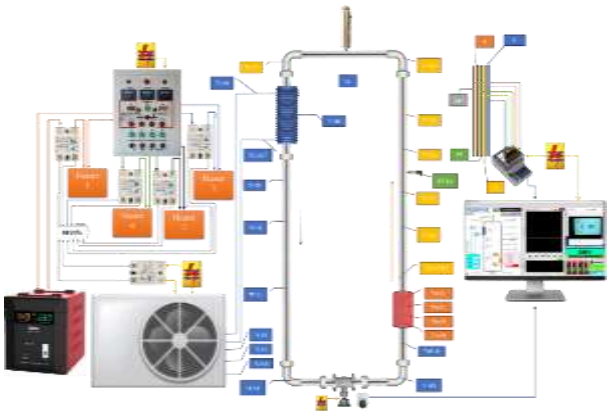

**Fig. 2.** I&C scheme of the FASSIP-05.

As part of the experiment, the cooler's temperature was initially lowered to its maximum limit, followed by the activation of the heater to establish an effective initial temperature gradient. The cooler operates at its maximum cooling capacity, and the heater was activated at its maximum power (4000 W). This process continues until the outlet temperature of the heater matches the set point temperature. To ensure the validity of the results, each set point temperature of 60 °C, 70 °C, 80 °C, and 90 °C is rigorously tested three times, as detailed in Table 1.

**Table 1.** FASSIP-05 Experimental Matrix.

| Set Point ( °C) | Cooler initial Temperature ( °C) | Repetition | Pressure (bar) | Inclination (°) |
|---|---|---|---|---|
| 60 | 17 | 3× | 1 | 0 |
| 70 | 17 | 3× | 1 | 0 |
| 80 | 17 | 3× | 1 | 0 |
| 90 | 17 | 3× | 1 | 0 |

Temperature data is collected using K-type thermocouples (%Error < 1%) with ½ inch threads connected to National Instruments 9213 and 9214 data acquisition systems. LabVIEW software monitors and records data via a Human Machine Interface (HMI) panel.

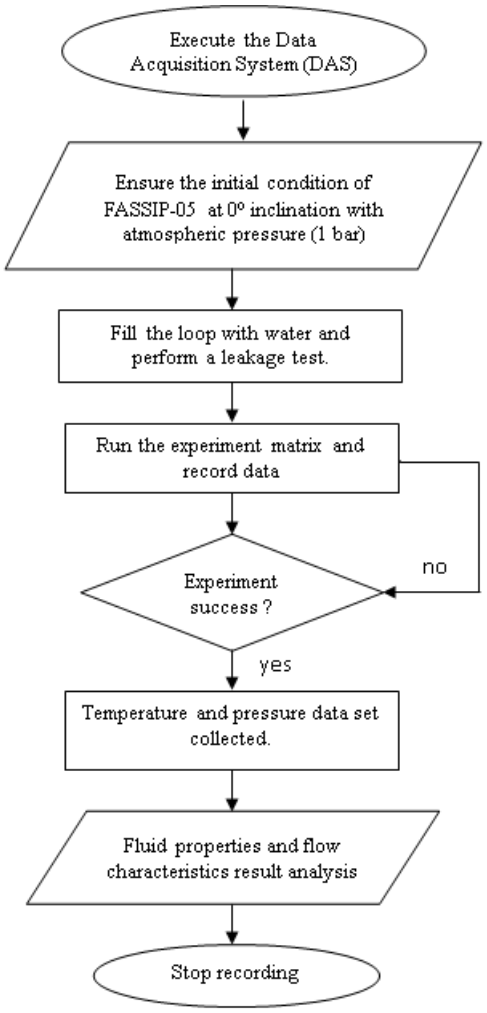


**Fig. 3.** Flowchart of Experimental FASSIP-05.

After reaching the set point temperature, the system wss maintained at the given temperature for 3 hours under steady-state conditions to ensure reliable data. The collected temperature readings were analyzed to determine the distribution along the loop, identifying natural circulation flow patterns and regimes, such as laminar, transitional, or turbulent flow. This analysis is crucial for understanding the phenomenon of the natural circulation loop under varying thermal conditions. The experimental results were compared with existing literature and previous studies to highlight the unique aspects of this research. One such aspect is the exclusion of a flow meter, which could be determined based on temperature and pressure changes. Another aspect is the use of pressurized working fluids. By following this methodology, the study aims to provide a comprehensive understanding of natural circulation flow regimes in passive cooling systems, contributing to advancing nuclear reactor safety and thermal management strategies.

### 3.2 Calculation data

The Grashof number (Gr) for natural circulation loops (NCL) is modified to account for specific parameters in the system [13].

$$Gr_m = \frac{\rho^2 \beta g q H D^3}{\mu^3 A c_p} \quad (1)$$

the modified Grashof number is indicated as $Gr_m$ (non-dimensional number), fluids density is $\rho$ (kg/m³), gravitational force is $g$ (m²/s), heater power $q$ (W), height difference is $H$ (m), inner pipe diameter is $D$ (m), dynamic viscosity is $\mu$ (kg/m.s), flow area is $A$ (m²), and specific heat is $c_P$ (kJ/kg°C). The thermal expansion $\beta$ (°C$^{-1}$) correlation is defined as follows [14]:

$$\beta = \frac{\rho_0 - \rho_1}{\rho_1 (T_1 - T_0)} \quad (2)$$

where initial temperature is $T_o$ (°C), final temperature is $T_I$ (°C), initial density is $\rho_0$ (kg/m³), and final density is $\rho_I$ (kg/m³). To obtain the physical properties of water, the data compiled by Crabtree & Siman-Tov (1993) was used, utilizing constants A, B, C, and D with different values for various property calculations [15]. The specific heat capacity ($c_p$) can be obtained as follows:

$$c_p = 1000 \times \left[\frac{A + CT}{1 + BT + DT^2}\right]^{1/2} \quad (3)$$

where **A** = 17.48908904, **B** = -1.67507 x 10$^{-3}$, **C** = -0.03189591, and **D** = -2.8748 x 10$^{-}$6. The dynamic viscosity, $\mu$ can be obtained by the following equation.

$$\mu = exp\left[\frac{A + CT}{1 + BT + DT^2}\right] \quad (4)$$

with **A** = -6.325203964, **B** = 8.705317 x 10$^{-3}$, **C** = -0.088832314, and **D** = -9.657 x 10$^{-7}$. Meanwhile, the water density ($\rho$) can be estimated using the following equation :

$$\rho = A + BT_F + CT_F^2 \quad (5)$$

Where temperature is $T$ (°C), $T_F$ = 1.8$T$ + 32, **A** = 1004.789042, **B** = -0.046283, and **C** = -7.9739 x 10$^{-4}$.

The steady-state Reynolds number can be determined using the correlation proposed by P.K. Vijayan in 2002 [16].

$$\mathbf{Re_{ss}} = C\left(\frac{Gr_m}{N_G}\right)^r \quad (6)$$

where $C = \left(\frac{2}{p}\right)^{1/(3-b)}$ and $r = 1/(3-b)$

while $p$ is the friction factor and $b$ is the exponent of the friction factor, for the exponent value of the friction factor in the laminar flow regime it is determined by the Blasius correlation of 1 and the friction factor constant of 64, for turbulence the value of b is 0.25 and p is 0.316.

Fully laminar flow:

$$Re = 0.1768\left[\frac{(Gr_m)}{N_G}\right]^{0.5} \quad (7)$$

Fully transient flow:

$$Re = 1.2161\left[\frac{(Gr_m)}{N_G}\right]^{1/2.584} \quad (8)$$

Fully turbulent flow:

$$Re = 1.96\left[\frac{(Gr_m)}{N_G}\right]^{1/2.75} \quad (9)$$

$N_G$ represents the geometric ratio calculated by dividing the total loop length by the inner diameter of the pipe.

Before calculating the mass flow rate, it is essential to determine the Darcy friction factor. The Darcy friction factor $f_D$ can be calculated using the Churchill correlation, which is applicable for a wide range of Reynolds numbers and pipe roughness values [17]:

$$f_D = 8\left[\left(\frac{8}{Re}\right)^{12} + \frac{1}{(A+B)^{3/2}}\right]^{1/12} \quad (10)$$

$$A = \left[2.457\, ln\left(\frac{1}{\left(\frac{7}{Re}\right)^{0.9} + 0.27\frac{\varepsilon}{D}}\right)\right]^{16} \quad (11)$$

$$B = \left(\frac{37530}{Re}\right)^{16} \quad (12)$$

where $f_D$ is Darcy friction factor, $D$ is Pipe diameter (m), $\varepsilon$ is pipe roughness (m).

Using the steady-state Reynolds number and the Darcy friction factor, the mass flow rate $W_{ss}$ (kg/s) can be derived from the balance of buoyancy and frictional forces:

$$\rho\beta g \Delta T V = \frac{R W_{ss}^2 A}{2\rho} \quad (13)$$

with $R = f_D L/DA^2$ ; $V = A.\Delta z$ ; $\Delta T = q_h/W_{ss}c_p$ ; $A = \pi D^2/4$. Consequently, the correlation is transformed.

$$W_{ss}^2 = \frac{2\rho^2\beta g\,(\frac{q_h}{W_{ss}c_p})A\Delta z}{\frac{f_D}{DA^2}A} \quad (14)$$

$$W_{ss}^3 = \frac{2\rho^2\beta g\,q_h\Delta z}{\frac{f_D L}{DA^2}c_p} \quad (15)$$

$$W_{ss} = \sqrt[3]{\frac{2\rho^2\beta g\,q_h\Delta z D A^2}{f_D L c_p}} \quad (16)$$

$$W_{ss} = \sqrt[3]{\frac{2\rho^2\beta g\,q_h\Delta z D\left(\pi D^2/4\right)^2}{f_D L c_p}} \quad (17)$$

$$W_{ss} = \frac{1}{2}\sqrt[3]{\frac{\rho^2\beta g\,q_h\Delta z D^5\pi^2}{f_D L c_p}} \quad (18)$$

Equation 18 shows the relationship between mass flow rate with density, thermal expansion, power, frictional factor, and geometrical parameters.

## 4. RESULTS AND DISCUSSION

The experimental results and calculations the understanding of the physical properties of water. These results, with a equation 3 – 5, are represented in Figures 4 – 6.

Figure 4 presents the relationship between temperature settings and density in both hot and cold legs. At a temperature setting of 60 °C, it reaches its peak density, registering at 986.87 kg/m3, with an average temperature of 50.93 °C. This observation suggests a critical point where the cold leg's density peaks at a particular temperature. In contrast, the hot leg shows an inverse correlation between temperature settings and density. At the temperature setting of 90 °C, it demonstrates its lowest density, recording at 966.23 kg/m3, with an average temperature of 89.33 °C.

Figure 5 elucidates the relationship between temperature setting variations and the dynamic viscosity of both hot and cold legs. The data demonstrates that the viscosity of both hot and cold legs decreases as the temperature setting increases. A notable observation is the peak viscosity dynamics at a temperature setting of 60 °C in the cold leg, where the average temperature registers at 50.93 °C, and the dynamic viscosity reaches 0.000537 kg/m.s. This peak indicates a critical point where the fluid's molecular interactions are most pronounced under these conditions, resulting in higher resistance to flow.

On the other hand, the lowest viscosity dynamics are recorded at a temperature setting of 90 °C in the hot leg. Here, the average temperature is 89.33 °C, and the dynamic viscosity drops to 0.000317 kg/m.s. This significant reduction in viscosity at higher temperatures underscores the decreased intermolecular forces, facilitating smoother fluid movement and lower resistance. Understanding the relationship between temperature and viscosity is crucial for optimizing fluid flow and enhancing system performance. By analyzing these viscosity dynamics, engineers can develop more efficient thermal management strategies and improve the operational efficiency of systems that rely on precise temperature control. Fig. 5, shows a detailed between temperature settings and dynamic viscosity, revealing critical patterns that important for better engineering practices and decision-making.

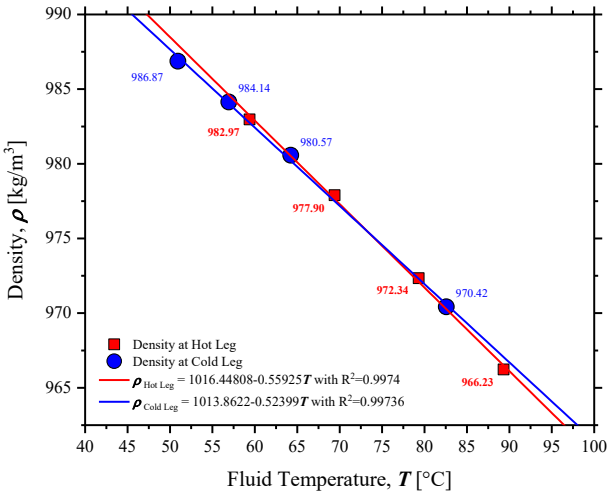


**Fig. 4.** Fluid density of NCL.

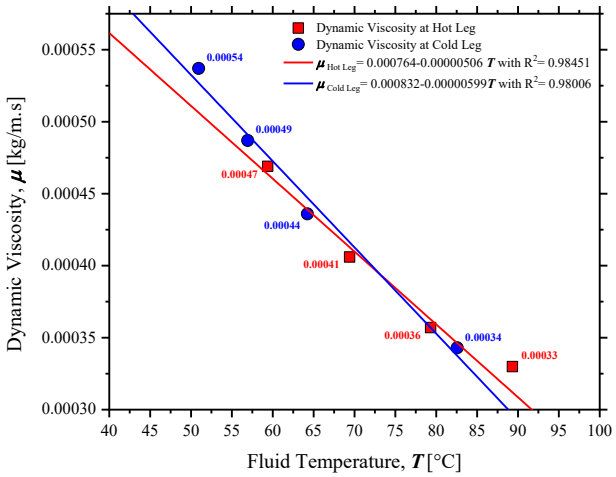


**Fig. 5.** Dynamic viscosity throughout the loop.

Figure 6 provides an illustration of the relationship between temperature setting variations and the specific heat of both hot and cold legs. The

specific heat capacity, which is the amount of heat required to raise the temperature of a unit mass of a substance by one degree Celsius, varies with temperature changes. The coldest specific heat value, recorded at 60 °C in the cold leg, with an average temperature of 50.93 °C and a specific heat of 4181.74 kJ/kg °C, suggests that the fluid requires less energy to increase its temperature under these conditions. Conversely, the highest specific heat, observed at 90°C in the hot leg, with an average temperature of 89.33°C and a specific heat of 4206.33 kJ/kg °C, indicates that the fluid's capacity to store thermal energy increases with temperature, requiring more energy to achieve the intended temperature change. These variations in specific heat shows the varying ability of the water to absorb and retain heat at different temperature points, a crucial factor in optimizing thermal management and system efficiency. Understanding these specific heat variations, provides valuable insights for designing and managing systems that rely on precise temperature control, ensuring optimal performance and energy utilization.

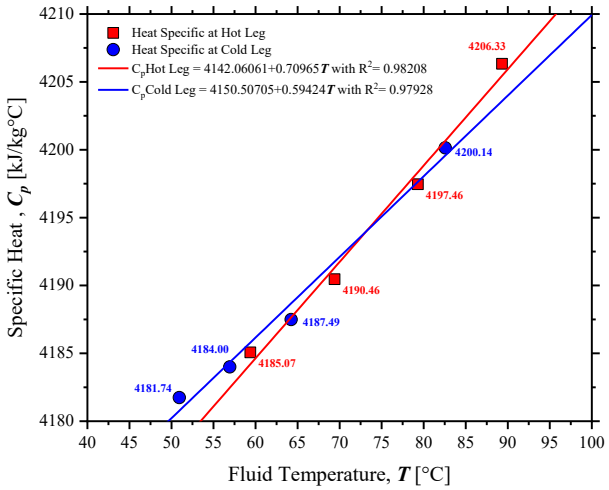


**Fig. 6.** Specific heat profile of FASSIP-05 working fluid.

Upon obtaining the computational results of the on the physical characteristics of water, the Grashof number can be calculated using Eq. 1. The calculated results are presented in Tables 2-5.

**Table 2.** Grashof number results at 60 °C.

| Run | Set Point ( °C) | Thermal expansion (/ °C) | Avg. $Gr_m$ |
|---|---|---|---|
| 1 | 60 | 0.0004019 | $2.49\times10^{12}$ |
| 2 | 60 | 0.0004019 | $2.48\times10^{12}$ |
| 3 | 60 | 0.0004019 | $2.48\times10^{12}$ |

**Table 3.** Grashof number results at 70°C.

| Run | Set Point ( °C) | Thermal expansion ( $°C^{-1}$) | Avg. $Gr_m$ |
|---|---|---|---|
| 1 | 70 | 0.0004303 | $4.06\times10^{12}$ |
| 2 | 70 | 0.0004303 | $4.04\times10^{12}$ |
| 3 | 70 | 0.0004303 | $4.04\times10^{12}$ |

**Table 4.** Grashof number results at 80°C.

| Run | Set Point ( °C) | Thermal expansion ( $°C^{-1}$) | Avg. $Gr_m$ |
|---|---|---|---|
| 1 | 80 | 0.0004592 | $6.29\times10^{12}$ |
| 2 | 80 | 0.0004592 | $6.29\times10^{12}$ |
| 3 | 80 | 0.0004593 | $6.28\times10^{12}$ |

**Table 5.** Grashof number results at 90°C.

| Run | Set Point ( °C) | Thermal expansion ( $°C^{-1}$) | Avg. $Gr_m$ |
|---|---|---|---|
| 1 | 90 | 0.0004885 | $9.42\times10^{12}$ |
| 2 | 90 | 0.0004885 | $9.42\times10^{12}$ |
| 3 | 90 | 0.0004887 | $9.40\times10^{12}$ |

To confirm the accuracy of the data presented in Table 2-5, a linear graph was created to show the relationship between the Grashof number and the temperature configuration. The averaged Grashof number values at each temperature setting are as follows: $2.48\times10^{12}$ at 60 °C, $4.04\times10^{12}$ at 70 °C, $6.29\times10^{12}$ at 80 °C, and $9.42\times10^{12}$ at 90 °C.

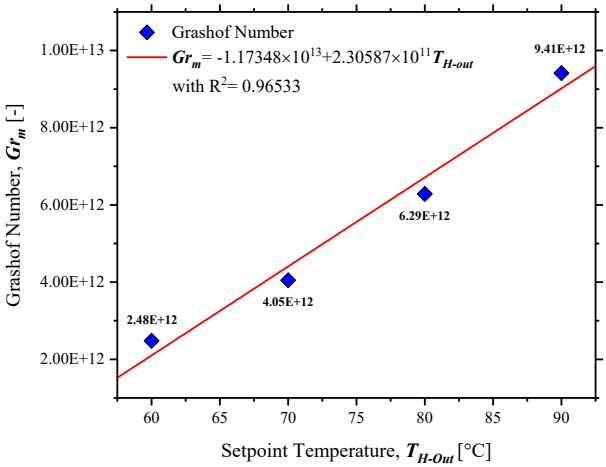


**Fig. 7.** Plot of Grashof number as a function of temperature.

Figure 7 illustrates a detailed graph of the Grashof number, presenting four distinct variations in temperature setpoints under steady-state conditions. The Grashof number, varies linearly with temperature, as indicated by an $R^2$ value of 0.96533. One of the significant findings from the adjusted Grashof analysis is the observation of a turbulent NCL flow regime across the specified temperature range, specifically around ($10^{12}$). This range indicates a regime where the flow transitions from

laminar to turbulent due to the increased buoyancy forces overcoming viscous forces. The turbulent flow regime is characterized by chaotic and irregular fluid motion, which enhances heat transfer and mixing within the system.

The Vijayan correlation (Eq. 9) is utilized in this study to determine the Reynolds number based on the flow regime indicated by the Grashof number for each temperature setpoint. This correlation provides a precise relationship between these two dimensionless parameters, enhancing the accuracy and reliability of this research.

$T_{H\text{-}out}$ 60 °C => $Re = 1.96 \left[\frac{2.48\times10^{12}}{482.859}\right]^{1/2.75}$ = 6664.5

$T_{H\text{-}out}$ 70 °C => $Re = 1.96 \left[\frac{4.04\times10^{12}}{482.859}\right]^{1/2.75}$ = 7966.92

$T_{H\text{-}out}$ 80 °C => $Re = 1.96 \left[\frac{6.29\times10^{12}}{482.859}\right]^{1/2.75}$ = 9338.07

$T_{H\text{-}out}$ 90 °C => $Re = 1.96 \left[\frac{9.42\times10^{12}}{482.859}\right]^{1/2.75}$ = 10820

During the experiment, stainless steel pipes were integrated into the FASSIP-05 system. The surface roughness was measured to be 0.046 mm. Figures 8-11 present a comprehensive analysis of the relationship between temperature and critical parameters within a NCL, specifically focusing on the steady-state mass flow rate and the Darcy friction factor. As depicted in these figures, an increase in temperature results in a corresponding rise in the steady-state mass flow rate. This increase indicates enhanced fluid circulation, improved thermal performance and more excellent stability within the system. The mass flow rate's stability at higher temperatures can be attributed to the intensified buoyancy forces, which drive the natural circulation more effectively.

Simultaneously, the figures reveal a notable decrease in the Darcy friction factor with increased temperatures. The Darcy friction factor, a dimensionless unit representing the resistance to flow within the loop, is influenced by various factors, including fluid viscosity and flow regime. As the temperature increases, the fluid's viscosity decreases, reducing the frictional resistance and thereby lowering the Darcy friction factor. This inverse relationship between temperature and the Darcy friction factor underscores the thermodynamic principles governing the NCL. The decrease in the Darcy friction factor at higher temperatures highlights the system's reduced energy losses due to friction, facilitating smoother and more efficient fluid flow. This reduction in frictional resistance is crucial in optimizing the loop's overall performance, as it enables the system to maintain higher flow rates with less energy input. Furthermore, the enhanced stability of the mass flow rate at elevated temperatures points to a more robust and reliable operation of the NCL, which is essential for applications requiring consistent and efficient thermal management.

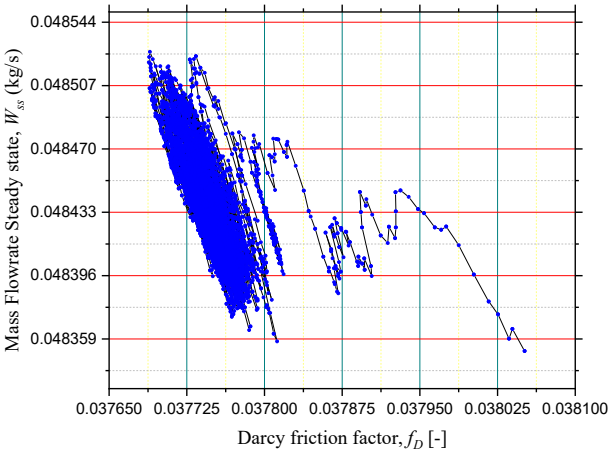


**Fig. 8.** Mass flow rate in steady state vs Darcy Friction Factor profile at 60 °C

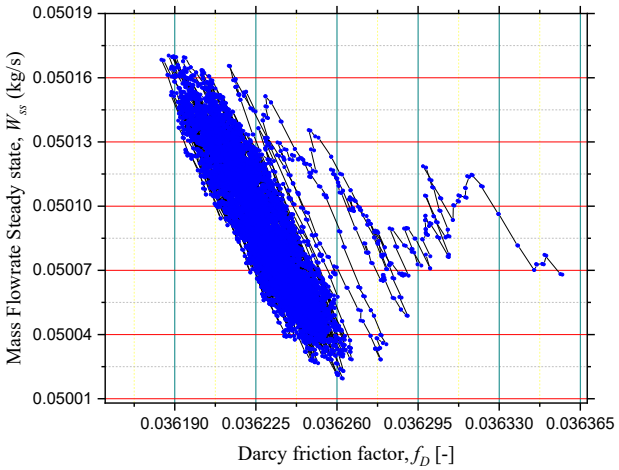


**Fig. 9.** Mass flow rate in steady state vs Darcy Friction Factor profile at 70 °C

NCL observations were also conducted on Reynolds steady-state numbers, revealing the resemblance of flow regimes to Grashof numbers. To substantiate this claim, $\mathbf{Re_{ss}}$ was examined by relating the average $\boldsymbol{W_{ss}}$ to $\boldsymbol{f_D}$ using the general equation $\mathbf{Re_{ss}} = {}^{W_{ss}D}/_{\mu A}$ and compared with another researches [18–22].

The turbulent flow observed in Fig. 12 illustrates a significant correlation between the values of Grashof's number and Reynolds' number across a range of temperatures. Furthermore, the inclusion of the Darcy Friction Factor resulted in a

reduction in Reynolds' number. Comparing these findings with those of other researchers establishes the presence of consistent turbulent regimes, although there are exceptions, such as Wang 2013 and Srivastava 2023, which exhibited laminar flow [18, 20]. The variations in Reynolds' number primarily arise from dissimilarities in each facility's geometric characteristics and research methodologies.

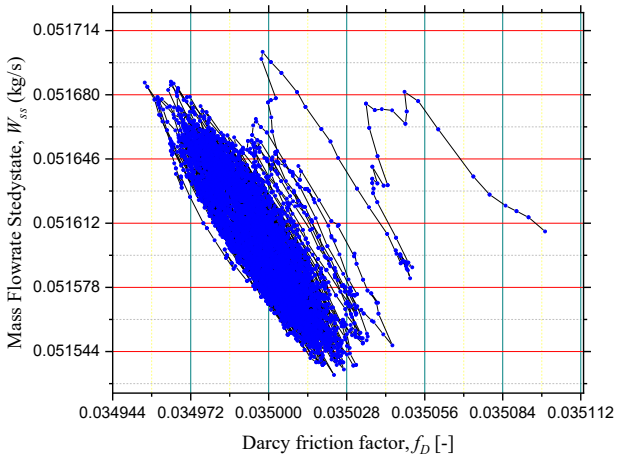


**Fig. 10.** Mass flow rate in steady state vs Darcy Friction Factor profile at 80 °C

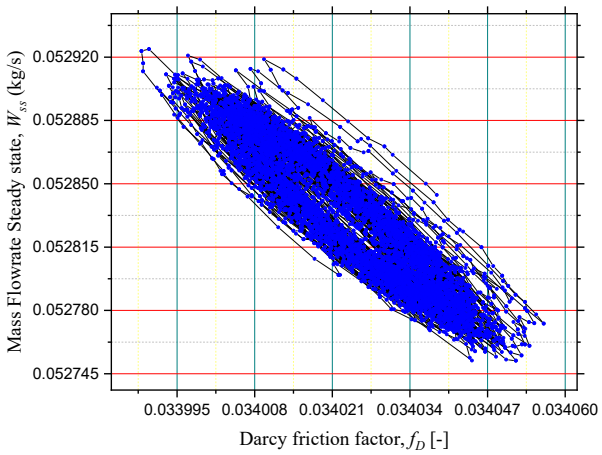


**Fig. 11.** Mass flow rate in steady state vs Darcy Friction Factor profile at 90 °C

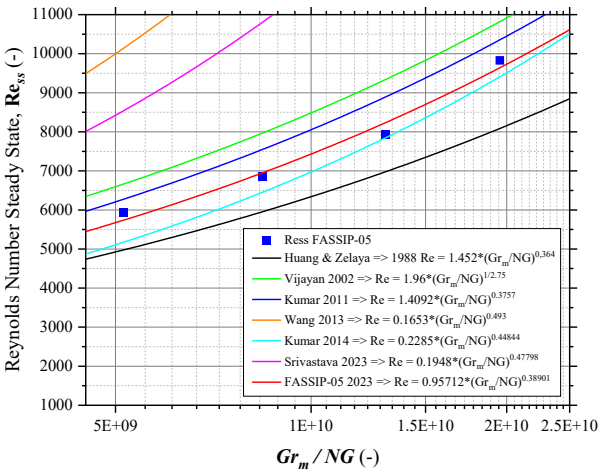


**Fig. 12.** Comparison of Reynolds number against $Gr_m/N_G$.

## 5. CONCLUSION

The experimental results underscore the practical implications of temperature on the physical properties of water and the natural circulation flow in a rectangular loop. The variations in density, viscosity, and specific heat with temperature directly impact the Grashof and Reynolds numbers, thereby influencing the flow regime. The calculated mass flow rates demonstrate that higher temperatures foster more robust natural circulation, a crucial finding for designing and optimizing passive cooling systems in nuclear reactors.

These findings have immediate practical implications for designing and optimizing passive cooling systems in nuclear reactors and significantly contribute to the broader understanding of natural circulation phenomena. This research is a crucial step towards developing more reliable and efficient passive cooling strategies.

## ACKNOWLEDGMENT

Acknowledgments were expressed to the *Program Riset dan Inovasi Indonesia Maju* (RIIM) Batch-1 of the Mandatory LPDP of the Ministry of Finance-BRIN from 2022 to 2025 under contract numbers B-811/II.7.5/FR/6/2022 and B-2103/III.2/HK.04.03/7/2022. Gratitude is extended to the Funding from "PRTRN-BRIN Rumah Program" with research proposal code D1463. Appreciation is also conveyed to the Head of the ORTN-BRIN Research Center for Nuclear Reactor Technology and all NRTFSys members.

## AUTHOR CONTRIBUTION

All authors have equally contributed as the primary contributors of this paper. The final version

of the paper has been thoroughly reviewed and approved by all authors.

## REFERENCES


1. Jabbari M., Hadad K., Pirouzmand A. Re-assessment of station blackout accident in VVER-1000 NPP with additional measures following Fukushima accident using Relap/Mod3.2. Annals of Nuclear Energy. 2019. **129**:316–30.
2. Anhar Riza Antariksawan, Mulya Juarsa Nuclear Reactor Safety: Basic Design Accidents and Severe Accidents (in Indonesian Language). First ed. Jakarta:BRIN; 2023.
3. IAEA *IAEA International Fact Finding expert mission of the Fukushima Dai-Ichi NPP accident following the Great East Japan Earthquake and Tsunami*. REPORT : THE GREAT EAST JAPAN EARTHQUAKE EXPERT MISSION. 2011.
4. Juarsa M., Antariksawan A.R., Kusuma M.H., Haryanto D., Putra N. Estimation of Natural Circulation Flow Based on Temperature in The FASSIP-02 Large-Scale Test Loop Facility. IOP Conference Series: Earth and Environmental Science. 2018. **105**(1)
5. Lesmana R.S., Juarsa M., Waskita A.A. Numerical Analysis Model on SinglePhase Natural Circulation in Fassip-01 Mod.1 Rectangular Loop Based on Heater Position (in Indonesian Language). Sigma Epsilon. 2019. **23**(2):70–8.
6. Juarsa M., Purba J.H., Kusuma H.M., Setiadipura T., Widodo S. Preliminary Study on Mass Flow Rate in Passive Cooling Experimental Simulation During Transient Using NC-Queen Apparatus. Atom Indonesia. 2014. **40**(3):141–7.
7. Tjahjono H. Comprehensive Prediction of Thermosyphon Characteristics in Reactor Passive Cooling System Simulation Loop FASSIP-01. Atom Indonesia. 2017. **43**(3):157–66.
8. Andrea S.A.A. *Analysis of Changes in Thermal Energy Based on Water Temperature Variations in the Heating Tank of FASSIP-02 Test Loop (in Indonesia Language)*.Universitas Andalas; 2022.
9. Haryanto D., Budiman A.A., Putra M.G., Setiawan P.H., Juarsa M. Investigation of Heat Exchanger Performance in The Heating Tank Section of Loop FASSIP 03 NT. Jurnal Teknologi. 2024. **16**(1):41.
10. Yuliaji D., Waluyo R., Pramono G.E., Setiawan P.H., Juarsa M. The Commissioning Test Facility of Passive Simulation System 04 Version 2 (FASSIP 04 VER.2) for Passive Cooling Capability Study on Nuclear Reactor Safety System (in Indonesian Language). Jurnal Ilmiah Teknik Mesin. 2023. **9**(1):57–63.
11. Adrian H., Roswandi I., Gunawan H.A., Sukarno R., Syaka D.R.B., Juarsa M. Estimated Calculation of Natural Circulation Flow Rate in the of Fassip-05 Pressurized Test Loop (In Indonesian Language). Jurnal Ilmiah Teknik Mesin. 2023. **9**(2):86–92.
12. Roswandi I., Gunawan H.A., Budiman A.A., Adrian H., Sanda, Juarsa M. Reliability Investigation of Heater and Cooler of Passive System Simulation Facility-05 (FASSIP-05) Based on Initial Commissioning Phase (in Indonesian Language). Jurnal Teknik Mesin Indonesia. 2023. **18**(2):15–20.
13. Pilkhwal D.S., Ambrosini W., Forgione N., Vijayan P.K., Saha D., Ferreri J.C. Analysis of the unstable behaviour of a single-phase natural circulation loop with one-dimensional and computational fluid-dynamic models. Annals of Nuclear Energy. 2007. **34**(5):339–55.
14. ToolBox T.E. *Volumetric (Cubic) Thermal Expansion* [Accessed: 30 April 2024]. Available from: https://www.engineeringtoolbox.com/volumetric-temperature-expansion-d_315.html.
15. Crabtree A., Siman-Tov M. *Thermophysical Properties of Saturated Light and Heavy Water for Advanced Neutron Source Applications*. United States: 1993.
16. Vijayan P.K. Experimental Observations on The General Trends of The Steady State and Stability Behaviour of Single-Phase Natural Circulation Loops. Nuclear Engineering and Design. 2002. **215**(1–2):139–52.
17. Churchill S.W. Friction Factor Equation Spans All Fluid-Flow Regimes. Chemical Engineering. 1977. **84**((24)):91–2.
18. Srivastava A.K., Saikrishna N., Maheshwari N.K. Steady State Performance of Molten Salt Natural Circulation Loop With Different Orientations of Heater and Cooler. Applied Thermal Engineering. 2023. **218**(September 2022):119318.
19. Kumar N., Doshi J.B., Vijayan P.K. Investigations on The Role of Mixed Convection and Wall Friction Factor in Single-Phase Natural Circulation Loop Dynamics. Annals of Nuclear Energy. 2011. **38**(10):2247–70.
20. Wang J.Y., Chuang T.J., Ferng Y.M. CFD Investigating Flow and Heat Transfer Characteristics in a Natural Circulation Loop. Annals of Nuclear Energy. 2013. **58**:65–71.
21. Hariyanto D., Permana S., Waris A., Mustari A.P.A., Kinoshita M., Aji I.K., et al. Irregular Pentagon Loop for Nuclear Reactor Natural Circulation System Test Apparatus. Nuclear Engineering and Design. 2024. **416**(November 2023):112753.
22. Naveen K., Iyer K.N., Doshi J.B., Vijayan P.K. Investigations on Single-Phase Natural Circulation Loop Dynamics. Part 2: Role of Wall Constitutive Laws. Progress in Nuclear Energy. 2014. **75**:105–16.